IMPERIAL

Imperial College London
Department of Mathematics

Sequential Monte Carlo Guided Diffusion Sampling for General Optimization

Brendan Dowling

CID: 02458886

Supervised by Dr Deniz O. Akyildiz

August 26, 2024

Submitted in partial fulfilment of the requirements for the MSc in Statistics at Imperial College London

The work contained in this thesis is my own work unless otherwise stated.

Signed: Brendan Dowling Date: August 26, 2024

Acknowledgements

I want to give special thanks to my supervisor, Dr Deniz Akyildiz, who has provided excellent guidance over the course of this work. The dedication of his time towards answering my questions and suggesting avenues to explore went beyond expectations and was greatly appreciated. I also want to thank Benjamin Boys for meeting with me several times, providing insightful and guiding discussions related to this research, and for providing access to his code. I also want to give special thanks to my family for their continued support of my studies and for providing me the resources needed to excel. Lastly, I want to thank my fiancée for her support over this challenging past year; without her this thesis could not have happened.

Abstract

Diffusion models have have been shown to learn underlying data distributions, even in high-dimensional settings as demonstrated by their state-of-the-art performance on image, video and molecular synthesis tasks. From a Bayesian perspective, this makes them suitable as prior models. Recent research has explored how to accurately *guide* the diffusion process for posterior sampling. Such methods have primarily focused on solving ill-posed inverse problems by approximating the time conditional score function to use in the reverse sampling steps. In this paper, we present a novel and general framework, `SMCDiffOpt`, for guiding diffusion models with sequential Monte Carlo methods. The framework considers inverse problems as a special case of optimization, where we've reframed the optimization task as a sampling problem from an annealed Boltzmann-Gibbs distribution defined by the objective, using the diffusion model as a prior. This framework can be applied even in settings where gradients are not available, making it both computationally efficient and applicable in black-box optimization settings. Relatedly, this framework does not necessitate conditional score approximations though can flexibly accommodate them for better sampling efficiency. We demonstrate the efficacy of the algorithm through experiments on synthetic and real-world inverse problems and optimization tasks.

Contents

1. Introduction

Score-based diffusion models (Ho et al., 2020; Sohl-Dickstein et al., 2015; Y. Song & Ermon, 2020) have garnered significant attention for their ability to model complex data distributions, particularly in high-dimensional spaces such as image (Dhariwal & Nichol, 2021; Rombach et al., 2021), video (Ho et al., 2022), and molecular (Xu et al., 2022) synthesis. These models operate by iteratively transforming noise into structured data, using a learned (Stein) score function, to effectively enable sampling from the underlying data distribution. Consequently, diffusion models have recently been considered as prior models for Bayesian posterior sampling tasks such as solving inverse problems (Y. Song & Ermon, 2020) and, more recently, optimisation (Guo et al., 2024; Kong et al., 2024; Krishnamoorthy et al., 2023).

There are roughly two core approaches to this posterior sampling task: training a conditional score network for the specific inverse problem (Nichol et al., 2021; Saharia et al., 2021, 2022; Y. Song & Ermon, 2020) or optimisation task (Guo et al., 2024; Krishnamoorthy et al., 2023); taking a pre-trained score network and guiding the generative process using approximations of the conditional score for inverse problems (Boys et al., 2023; Chung et al., 2022; J. Song et al., 2023) or gradients of the objective for optimisation (Kong et al., 2024). We focus on the latter approach since it enables zero shot inference — we can take any diffusion model and use it for any inverse/optimisation tasks without needing access to labelled samples.

We can view inverse problems as a special case of optimisation where the objective is the posterior density (i.e. maximum *a posteriori* estimation of the state (data) from the

observations/conditioning variable). Hence, through the optimisation lens, we may view the prior diffusion model as imposing constraints on the optimisation procedure. These constraints ensure that outcomes of the optimisation procedure lie on or near the data manifold, representing realistic configurations (Kong et al., 2024).

Recent work has considered using sequential Monte Carlo (SMC) methods (Chopin & Papaspiliopoulos, 2020) to correct for the approximation errors incurred during the guiding process (Cardoso et al., 2023; Dou & Song, 2023; Trippe et al., 2023; Wu et al., 2023). However, such frameworks have strictly focused on solving linear inverse problems. In this paper, we introduce `SMCDiffOpt`, a versatile framework that combines diffusion models with SMC methods to address both general optimization and inverse problems. Our framework views optimization as a posterior sampling problem from an annealed Boltzmann distribution, using diffusion models as priors and employing SMC methods to more effectively target the posterior distribution. It's also flexible, operating in zero-shot, accommodating different proposal distributions, and being able to operate without access to gradients of the objective — this makes it particularly effective in black-box optimization settings where only function evaluations are possible.

We contrast `SMCDiffOpt` with standard gradient-based optimizers on a synthetic optimisation task, highlighting its advantage at navigating complex optimization landscapes, including those with multiple optima. We also test it on the real-world SuperConductor black-box optimisation task (Trabucco et al., 2022), benchmarking it against other state-of-the-art approaches. Additionally, we demonstrate its performance and flexibility in solving inverse problems by comparing its posterior sampling efficiency to alternative methods on a synthetic Gaussian mixture model example.

The paper is organized as follows: Section 2 reviews the relevant background on optimization, inverse problems, diffusion models, and SMC methods, as well as mentioning some related and alternative approaches. Section 3 introduces the `SMCDiffOpt` framework, detailing its application to both general optimization tasks and inverse problems. Section 4 presents experimental results, and Section 5 discusses the broader implications of our findings and suggests directions for future research.

2. Background

2.1. Inverse Problems

Definition 2.1.1 (Inverse Problem with Gaussian Noise)**.** Given a data-point $\mathbf{x} \in \mathcal{X} \subseteq \mathbb{R}^{d_x}$, denote some lossy measurement by

$$\mathbf{y} = m(\mathbf{x}) + \sigma_y \epsilon \in \mathcal{Y}, \quad \epsilon \sim \mathcal{N}\left(0, \mathbf{I}_{d_y}\right) \tag{1}$$

where $m : \mathcal{X} \to \mathcal{Y} \subseteq \mathbb{R}^{d_y}$ is some *measurement operator*, and $\sigma_y \in \mathbb{R}^+$ controls the measurement noise. The goal of an inverse problem is to recover $\mathbf{x}$ from $\mathbf{y}$. We call $\mathcal{X}$ the *state space* and $\mathcal{Y}$ the *measurement space*.

Definition 2.1.2 (Linear Inverse Problem)**.** A linear inverse problem is an inverse problem where the measurement operator is such that $h(\mathbf{x}) = A\mathbf{x}$ for some matrix $A \in \mathbb{R}^{d_y \times d_x}$ called the *measurement matrix*.

Example 2.1.1 (Gaussian Deblurring)**.** Suppose we have some $\mathbf{x}$ representing a flattened $h \times w$ image (ignoring channels for simplicity). Let $h(\mathbf{x})$ represent the convolution of $\mathbf{x}$ with a Gaussian kernel. Given the discrete nature of images, this kernel can be represented as a $k \times k$ matrix. Given that the convolution operator is linear, we can form some matrix A from the kernel matrix (by using it to form a block Toeplitz matrix) so that $h(\mathbf{x}) = A\mathbf{x}$. It follows that if we have some blurry image, $\mathbf{y}$, generated according to Equation 1, the goal of inferring the unblurred image, $\mathbf{x}$, represents a linear inverse problem.

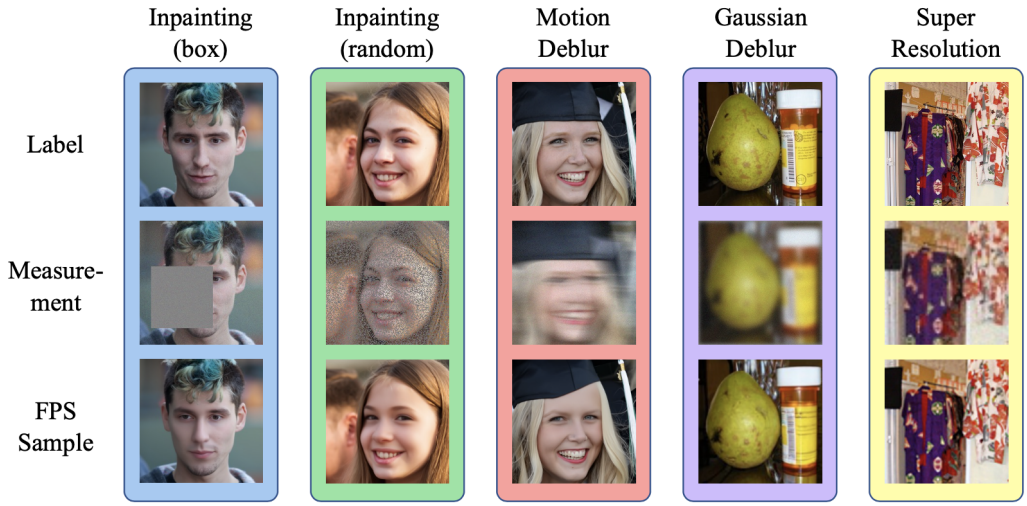

Figure 2.1.: Examples of inverse problems for image data (Dou & Song, 2023).

Remark 2.1.1 (Bayesian Solution to Ill-posed Inverse Problems)**.** Typically $d_x > d_y$, leading to a many-to-one $\mathbf{x} \to \mathbf{y}$ mapping (Chung et al., 2022), and requiring some *prior* information about $\mathbf{x}$. We call such an inverse problem *ill-posed*. If we assume some prior distribution of the data, $p(\mathbf{x})$, "solving" the inverse problem amounts to sampling from some posterior:

$$p(\mathbf{x} \mid \mathbf{y}) \propto p(\mathbf{x})g(\mathbf{y} \mid \mathbf{x}) = p(\mathbf{x})\mathcal{N}\left(\mathbf{y} \mid m(\mathbf{x}), \sigma_y^2 \mathbf{I}_{d_y}\right)$$

For many problems, $p(\mathbf{x})$ is generally unknown or does not conjugate with $g(\mathbf{y} \mid \mathbf{x})$, necessitating numerical methods to sample from $p(\mathbf{x} \mid \mathbf{y})$.

2.2. General Optimisation through Sampling

Definition 2.2.1 (Gibbs Measure / Boltzmann Distribution)**.** Let $\mathcal{X} \subseteq \mathbb{R}^{d_x}$ be a state space and let $h : \mathcal{X} \to \mathbb{R}$ be a measurable function, called the *energy function* or

Hamiltonian. The Gibbs measure is the probability density function over $\mathcal{X}$ given by:

$$q(\mathbf{x}; \beta) = \frac{\exp\{-\beta h(\mathbf{x})\}}{Z(\beta)} \tag{2}$$

where $\beta > 0$ is the *inverse temperature* parameter and $Z(\beta)$ is the normalizing constant (also known as the partition function), defined by:

$$Z(\beta) = \int_{\mathcal{X}} \exp\{-\beta h(\mathbf{x})\}\, d\mathbf{x}$$

Proposition 2.2.1 (Optimization via Sampling (Hwang, 1980; Kong et al., 2024))**.** Assume $h \in \mathrm{C}^3(\mathbb{R}^{d_x}, \mathbb{R})$ with $\{\mathbf{x}_i^*\}_{i=1}^M$ the set of its minimizers. Let p be a density on $\mathbb{R}^d$ such that there exists $i_0 \in \{1, \ldots, M\}$ with $p(\mathbf{x}_{i_0}^*) > 0$. Then Q_β, the distribution with density w.r.t the Lebesgue measure $\propto q(\mathbf{x}; \beta)p(\mathbf{x})$, weakly converges to Q_∞ as $\beta \to \infty$ and we have that:

$$Q_\infty = \frac{\sum_{i=1}^M a_i \delta_{\mathbf{x}_i^*}}{\sum_{i=1}^M a_i} \tag{3}$$

with $a_i = p(\mathbf{x}_i^*) \det(\nabla^2 h(\mathbf{x}_i^*))^{-1/2}$

Remark 2.2.1 (Annealing)**.** Proposition 2.2.1 tells us that by properly *tempering* β (i.e. slowly increasing it), we can globally optimize (minimize or maximize via negation) the function h. Note here that because β is the *inverse* temperature, we refer to increasing it as *annealing* (lowering the temperature). The density function p can be interpreted as some *prior* distribution we use to sample the points $\mathbf{x}$ (ideally such that more 'mass' is placed near the optima, $\{\mathbf{x}_i^*\}_{i=1}^M$, *a priori*).

2.3. Diffusion Models

Definition 2.3.1 (Stein Score)**.** Given a probability density function $p(\mathbf{x})$ on $\mathbb{R}^{d_x}$, the Stein score function is given by $\nabla_{\mathbf{x}} \log p(\mathbf{x})$, the gradient of the log-density with respect

to the data (*not* the distribution's parameters). Going forwards, we refer to the Stein score simply as the *score*, in-line with convention in related literature.

Definition 2.3.2 (Forwards Noising Process (Dou & Song, 2023))**.** Let $\mathbf{x}_0$ be a sample from some p_{data} distribution. Define the *forward noising process* as a Markov chain:

$$q(\mathbf{x}_{1:T} \mid \mathbf{x}_0) = \prod_{t=1}^{T} \mathcal{N}\left(a_t \mathbf{x}_{t-1}, b_t^2 \mathrm{I}_{d_x}\right)$$

where $\{(a_t, b_t)\}_{t=1}^T$ differ depending on formulation of the problem, and T is typically quite large (≈ 1000). a_t and b_t can be interpreted as the *memory retention factor* and *noise magnitude* of the forward process which typically decrease and increase, respectively, with time.

Definition 2.3.3 (Forward Marginal (Dou & Song, 2023))**.** Given some forward noising process defined by $\{(a_t, b_t)\}_{t=1}^T$, the *forward marginal* is given by:

$$q(\mathbf{x}_t \mid \mathbf{x}_0) = \mathcal{N}(c_t \mathbf{x}_0, d_t^2 \mathrm{I}_{d_x})$$

where c_t, d_t are derived from a_t and b_t. c_t essentially represents the signal strength (from the original sample) while d_t represents the cumulative noise. It follows that we should have $c_T \approx 0, d_T \approx 1$ since the goal is to fully destructure the data into $\mathcal{N}(0, \mathbf{I}_{d_x})$ noise.

Definition 2.3.4 (Backwards Denoising Process (Dou & Song, 2023))**.** Given some forward noising process, we assume[1] some backwards process ($t = T \to 0$) to be likewise a Markov chain with one-step backwards transition kernel given by:

$$p(\mathbf{x}_{t-1} \mid \mathbf{x}_t) = \mathcal{N}\left(u_t \cdot \hat{\mathbf{x}}_0(\mathbf{x}_t) + v_t \nabla_{\mathbf{x}_t} \log q(\mathbf{x}_t), w_t^2 \mathrm{I}_{d_x}\right) \tag{4}$$

[1]This assumption is well-founded for large T since the forward processes associated SDE (see Remark D.1) can be analytically reversed using the score thanks to the result of Anderson (1982). This, along with reducing the discretisation error of sampling from the SDE, is why we take T as large as feasible.

with u_t, v_t some functions of a_t, b_t, $q(\mathbf{x}_t) = \int q(\mathbf{x}_t \mid \mathbf{x}_0)p(\mathbf{x}_0)\, d\mathbf{x}_0$, and:

$$\hat{\mathbf{x}}_0(\mathbf{x}_t) := \mathbb{E}\left\{\mathbf{x}_0 \mid \mathbf{x}_t\right\} = \frac{\mathbf{x}_t + d_t^2 \nabla_{\mathbf{x}_t} \log q(\mathbf{x}_t)}{c_t} \tag{5}$$

derived from Tweedie's formula.

Remark 2.3.1 (DDPM Representation)**.** Under the de-noising diffusion probabilistic model (DDPM) of Ho et al. (2020), we take:

$$a_t = \sqrt{\alpha_t} \quad b_t = \sqrt{\beta_t} \quad c_t = \sqrt{\overline{\alpha}_t} \quad d_t = \sqrt{1 - \overline{\alpha}_t} \tag{6}$$

and

$$u_t = \sqrt{\overline{\alpha}_{t-1}}^2 \quad v_t = -\sqrt{\alpha_t}(1 - \overline{\alpha}_{t-1}) \quad w_t = \sqrt{\beta_t \cdot \frac{1 - \overline{\alpha}_{t-1}}{1 - \overline{\alpha}_t}} \tag{7}$$

with $\alpha_t = 1 - \beta_t$, for some $\beta_t \in (0, 1)$ known as the *noise schedule*, and $\overline{\alpha}_t = \prod_{\tau=1}^{t} \alpha_\tau$. For this paper, we primarily consider the DDPM formulation for simplicity. However, other formulations, such as de-noising diffusion implicit models (DDIM) of J. Song et al. (2020) (see Remark D.2) and Predictor-Corrector (PC) Y. Song et al. (2021), are equally applicable to our proposed framework; the only requirement is that the formulations conform to the above representations of the forwards and backwards process, and enable sampling at discrete time points.

Remark 2.3.2 (Noise Schedule)**.** Under the DDPM framework, the core parameter to tune is the noising schedule, β_t. Typically, we take this as an increasing function from some very low $\beta_{\min}$ to some $\beta_{\max}$. A linear schedule is the obvious and common choice, but other schedules, such as the cosine schedule of Nichol and Dhariwal (2021), can lead to better sampling performance. For this paper, the exact details of the schedule are not of significant importance; for experiments we use the linear schedule.

Proposition 2.3.1 (Score to Noise Conversion)**.** Let $\mathbf{x}_t = c_t\mathbf{x}_0 + d_t\epsilon_t$ be a forward noised

[2] In Dou and Song (2023) this is incorrectly given as $\sqrt{\alpha_{t-1}}$.

observation. Then

$$\nabla_{\mathbf{x}_t} \log q_t(\mathbf{x}_t) \approx -\frac{\epsilon_t}{d_t}.$$

Proof. Follows from forward marginal and Tweedie's formula (Equation 5). □

Given Definition 2.3.4 (and Proposition 2.3.1), it follows that if we have access to the score (or noise added), we can sample from p_{data} by sampling $\mathbf{x}_T \sim \mathcal{N}(0, \mathbf{I}_{d_x})$ ($\approx q(\mathbf{x}_T \mid \mathbf{x}_0)$) and iterating backwards in time according to Equation 4 until $t = 0$.

Unfortunately, $\nabla_{\mathbf{x}_t} \log q(\mathbf{x}_t)$ is intractable[3]. As such, we train a score-approximating (Y. Song et al., 2021) (or noise-predicting (Ho et al., 2020), and apply Proposition 2.3.1) neural network, denoted $s_\theta(\mathbf{x}_t, t)$ ($\epsilon_\theta(\mathbf{x}_t, t)$). We defer to the extensive literature (foundationally Ho et al. (2020), Y. Song and Ermon (2020), Y. Song et al. (2021) and Nichol and Dhariwal (2021)) on how precisely to train such a network, but generally this is achieved via minimization of a "re-weighted variant of the evidence lower bound" (Y. Song et al., 2021); e.g. for a score network:

$$\theta^* = \arg\min_\theta \sum_{t=1}^{T} (1 - \alpha_t) \mathbb{E}_{\mathbf{x}_0 \sim \hat{p}_{\text{data}}} \mathbb{E}_{\mathbf{x}_t \mid \mathbf{x}_0 \sim q_{\alpha_t}} \left[\| s_\theta(\mathbf{x}_t, t) - \nabla_{\mathbf{x}_t} \log q_{\alpha_t}(\mathbf{x}_t \mid \mathbf{x}_0) \|_2^2 \right]$$

where $\hat{p}_{\text{data}}$ is the empirical data distribution (i.e. based on our training samples), and q_{α_t} is the forward marginal at time t.

Plugging in this score network to Equation 4, we yield an approximate *backwards transition kernel*, $p_\theta(\mathbf{x}_{t-1} \mid \mathbf{x}_t) \approx q(\mathbf{x}_{t-1} \mid x_t)$, which we use to sample backwards in time. Formally, we sample according to:

$$p_\theta(\mathbf{x}_0) = \int p(\mathbf{x}_T) \prod_{t=1}^{T} p_\theta(\mathbf{x}_{t-1} \mid \mathbf{x}_t) \, d\mathbf{x}_{1:T}, \quad p(\mathbf{x}_T) = \mathcal{N}(\mathbf{x}_T; 0, \mathbf{I}_{d_x}) \tag{8}$$

[3] Note this is not $\nabla_{\mathbf{x}_t} \log q(\mathbf{x}_t \mid \mathbf{x}_0)$, which is tractable but "useless" for sampling since we don't know $\mathbf{x}_0$ a priori (it's what we're trying to sample); this quantity is useful, however, for training where we *do* know $\mathbf{x}_0$.

with, given a well trained network, $p_\theta(\mathbf{x}_0) \approx p_{\text{data}}(\mathbf{x}_0)$. Denote the mean of this transition kernel by $\mu_t(\mathbf{x}_t, \theta)$ and the variance by Σ_t. For DDPM, we have:

$$\mu_t(\mathbf{x}_t, \theta) = \frac{1}{\sqrt{\alpha_t}}\mathbf{x}_t + \frac{\beta_t}{\sqrt{\alpha_t}} s_\theta(\mathbf{x}_t, t) \tag{9}$$

$$\Sigma_t = \frac{\beta_t(1 - \overline{\alpha}_{t-1})}{1 - \overline{\alpha}_t} \cdot \mathbf{I} \tag{10}$$

2.4. Sequential Monte Carlo

Definition 2.4.1 (State Space Model)**.** Let $\mathbf{x}_t \in \mathcal{X}$ be a *state vector* at time t, which encapsulates all the information about some system necessary to predict future states (perhaps stochastically). Let $\mathbf{y}_t \in \mathcal{Y}$ be some observation vector at time t, representing (potentially noisy) measurements of the system. Let $\phi : \mathcal{X} \to \mathcal{X}$ be some function we call the *transition function*. Let $m : \mathcal{X} \to \mathcal{Y}$ be a measurement operator. Then the following dynamical system represents a (Gaussian) *state space model* (SSM):

$$\mathbf{X}_t \mid \mathbf{X}_{t-1} = \mathbf{x}_{t-1} \sim \mathcal{N}(\phi(\mathbf{x}_{t-1}), \sigma_x^2 \mathbf{I}_{d_x}) \tag{11}$$

$$\mathbf{Y}_t \mid \mathbf{X_t} = \mathbf{x}_t \sim \mathcal{N}(m(\mathbf{x}_t), \sigma_y^2 \mathbf{I}_{d_y}) \tag{12}$$

We refer to Equation 11 as the *transition kernel*, with density $f(\mathbf{x}_t \mid \mathbf{x}_{t-1})$, and Equation 12 as the *likelihood*, with density $g(\mathbf{y}_t \mid \mathbf{x}_t)$.

Definition 2.4.2 (Bayesian Filtering)**.** Suppose we have access to measurements $\mathbf{y}_{0:t}$ emitted from some SSM. The task of using such measurements to infer the hidden states, $\mathbf{x}_{0:t}$, is known as *Bayesian filtering*. We may be interested in the *joint filtering distribution*, with density $p(\mathbf{x}_{0:t} \mid \mathbf{y}_{0:t})$, or the *filtering distribution*, with density $p(\mathbf{x}_t \mid \mathbf{y}_{0:t})$. Focusing on the latter, given the setup of Definition 2.4.1, we can derive the

two-step recursive relationship:

$$\begin{aligned} p(\mathbf{x}_t \mid \mathbf{y}_{0:t-1}) &= \int p(\mathbf{x}_t, \mathbf{x}_{t-1} \mid \mathbf{y}_{0:t-1})\, d\mathbf{x}_{t-1} \\ &= \int f(\mathbf{x}_t \mid \mathbf{x}_{t-1}) p(\mathbf{x}_{t-1} \mid \mathbf{y}_{0:t-1})\, d\mathbf{x}_{t-1} \end{aligned} \tag{13}$$

$$\begin{aligned} p(\mathbf{x}_t \mid \mathbf{y}_{0:t}) &\propto p(\mathbf{x}_t, \mathbf{y}_t \mid \mathbf{y}_{0:t-1}) \\ &\propto p(\mathbf{x}_t \mid \mathbf{y}_{0:t-1}) g(\mathbf{y}_t \mid \mathbf{x}_t) \end{aligned} \tag{14}$$

Generally, however, the integral in Equation 13 and normalising constant in Equation 14 are intractable, necessitating approximate methods.

Definition 2.4.3 (Sequential Monte Carlo for Filtering[4])**.** Sequential Monte Carlo (SMC) provides a method for approximately sampling from the sequence of distributions as described in Definition 2.4.2 (Chopin & Papaspiliopoulos, 2020). It works by generating N particles, $\{\mathbf{x}_t^{(i)}\}_{i=1}^N$, according to some initial distribution, $r_0(\cdot)$, moving them according to some *proposal distribution*, $r_t(\cdot \mid \mathbf{x}_{t-1}, \mathbf{y}_t)$, weighting the particles according to some weighting function, $\omega_t(\mathbf{x}_t, \mathbf{x}_{t-1}, \mathbf{y}_t)$, and resampling[5] the particles according to their (self-normalised) weights $(W_t^{(i)})$. That is, the algorithm takes the following steps from $t = 1, \ldots, T$:

- **Propose**: $\tilde{\mathbf{x}}_t^{(i)} \sim r_t(\cdot \mid \mathbf{x}_{t-1}^{(i)}, \mathbf{y}_t), \quad i = 1, \ldots, N$
- **Weight**: $W_t^{(i)} \leftarrow\!\shortmid\, \omega_t^{(i)} \leftarrow \omega_t(\tilde{\mathbf{x}}_t^{(i)}, \mathbf{x}_{t-1}^{(i)}, \mathbf{y}_t) \quad i = 1, \ldots, N$
- **Resample**: $\{\mathbf{x}_{0:t}^{(i)}\}_{i=1}^N \sim \text{Multinomial}\left(\{\tilde{\mathbf{x}}_{0:t}^{(i)}\}_{i=1}^N; \{W^{(i)}\}_{i=1}^N\right)$

At the last step, we can yield an empirical distribution over the particles:

$$\hat{p}(\mathbf{x}_T \mid \mathbf{y}_{0:T}) = \sum_{i=1}^N W_T^{(i)} \delta_{\mathbf{x}_T^{(i)}(\mathbf{x}_T)}$$

[4] Also known as Particle Filtering.

[5] We present multinomial resampling for simplicity, but in practice alternative methods, such as systematic resampling, are used due to inefficiencies in the multinomial scheme (Chopin & Papaspiliopoulos, 2020)

which asymptotically (in N) approximates the true posterior distribution, $p(\mathbf{x}_T \mid \mathbf{y}_{0:T})$ (Chopin & Papaspiliopoulos, 2020; Del Moral, 2011).

Remark 2.4.1 (Weight Function)**.** The weight function's purpose is to correct for discrepancies between the proposal and true posterior, $p(\mathbf{x}_t \mid \mathbf{x}_{t-1}, \mathbf{y}_t)$, which it aims to approximate. In the filtering case for an SSM as in Definition 2.4.1, the weight function is given by the ratio of the two (Chopin & Papaspiliopoulos, 2020):

$$\omega_t^{(i)} = \frac{p(\tilde{\mathbf{x}}_t^{(i)} \mid \mathbf{x}_{t-1}^{(i)}, \mathbf{y}_t)}{r_t(\tilde{\mathbf{x}}_t^{(i)} \mid \mathbf{x}_{t-1}^{(i)}, \mathbf{y}_t)} \propto \frac{f(\tilde{\mathbf{x}}_t \mid \mathbf{x}_{t-1}^{(i)}) g(\mathbf{y}_t \mid \tilde{\mathbf{x}}_t^{(i)})}{r_t(\mathbf{x}_t \mid \mathbf{x}_{t-1}, \mathbf{y}_t)} \tag{15}$$

Remark 2.4.2 (Resampling)**.** The purpose of resampling is to avoid the issue of weight-degeneracy. Without resampling, after several iterations (i.e. for large T), most particles will end up having negligible weight (since without resampling we need to multiply all previous weights for the particle to get its time t weight) and eventually a single particle will dominate the approximation. Without resampling, we would not get the desired asymptotic results.

2.5. Related Work

The goal of conditionally sampling from p_{data} (learnt via a diffusion model) based on some $\mathbf{y}$ has been the center of significant recent research. The principle approach of most methods is to approximate $\nabla_{\mathbf{x}_t} \log q(\mathbf{x}_t \mid \mathbf{y})$, and plug this in to Equation 4 in place of its unconditional counterpart. The obvious approach is to train a conditional model to learn some $s_\theta(\mathbf{x}_t, \mathbf{y}, t)$ and use this. Indeed, this is the approach that modern text-to-image, image-to-image, and image-to-video applications take (Li et al., 2023; Nichol et al., 2021; Rombach et al., 2021; Saharia et al., 2021). This approach generally achieves the best conditional sampling but is limited in application; it requires training a model specific to each particular inverse problem (of which the aforementioned are examples)

which may be costly. Furthermore, such training requires having labelled data which may impose limitations in certain settings and for certain tasks.

A separate branch of research, and the area with which this work aligns, considers taking a pre-trained *unconditional* diffusion model (i.e. one where we just have a parametrised estimator of $\nabla_{\mathbf{x}_t} \log q(\mathbf{x}_t)$) and *guide* the diffusion process to enable conditional sampling. This is typically achieved by exploiting the following relationship:

$$\nabla_{\mathbf{x}_t} \log p_t(\mathbf{x}_t \mid \mathbf{y}) = \nabla_{\mathbf{x}_t} \log p_t(\mathbf{x}_t) + \nabla_{\mathbf{x}_t} \log p_t(\mathbf{y} \mid \mathbf{x}_t) \tag{16}$$

Replacing the first term with our pre-trained score network, optimal guidance can be achieved then by well-approximating $\nabla_{\mathbf{x}_t} \log p_t(\mathbf{y} \mid \mathbf{x}_t)$ (which is intractable). Such approximation methods are generally non-specific to the inverse problem, enabling taking any unconditional diffusion model and using it to sample from the desired posterior distribution. The diffusion-posterior-sampling method of Chung et al. (2022) was foundational, and can be applied to solve general inverse problems. J. Song et al. (2023) and, recently, Boys et al. (2023) have iterated on this with more analytically refined[6] approaches (though these are only applicable to linear inverse problems).

Given the difficulty of such approximations, and the sequential nature of the sampling procedure from diffusion models, significant recent research (Cardoso et al., 2023; Dou & Song, 2023; Janati et al., 2024; Trippe et al., 2023; Wu et al., 2023) has considered using SMC methods (with time running from $t = T \to 0$) to instead more directly target the posterior (or rather, the intermediate distributions $p(\mathbf{x}_t \mid \mathbf{y})$) and circumvent the need to compute this term. Our framework is most heavily inspired by the scheme of Cardoso et al. (2023); in Section 3.3 we demonstrate how their scheme is very closely related to our framework. In fact, each of these methods can be applied under our framework since their differences essentially lie primarily in their choice of proposal distribution.

However, our framework is generalised to solving any optimization task (not just inverse problems). Through this lens, our framework's objective and formulation aligns with

[6] See Boys et al., 2023 Section 5 for an excellent summary of how the methods co-relate.

that of Kong et al., 2024, with both employing Proposition 2.2.1 and essentially targeting the distribution induced by the diffusion model and the objective's associated annealed Boltmann distribution. However, where they guide the diffusion based on the score of the objective (with further corrections via Metropolis-adjusted Langevin dynamics), we instead use interacting particle systems (i.e. SMC). This circumvents the need to compute gradients of the objective function, making our method even better suited to black-box optimization tasks since it removes the need to train a surrogate model.

3. SMC-Guided Conditional Diffusion Sampling

3.1. `SMCDiffOpt` for General Optimization Problems

Consider some function $f : \mathcal{X} \to \mathbb{R}$ whose minima, $\{\mathbf{x}_i^*\}_{i=1}^M$, we wish to find. Consider $q(\mathbf{x}; \gamma) \propto \exp\{-\gamma f(\mathbf{x})\}$. Suppose we have some pre-trained score network which we can use to sample from p_{data} via some p_θ in T time-steps. Take p_θ as a prior for use in Proposition 2.2.1. Write $\mathbf{x}_0 := \mathbf{x}$. Naieve targeting of $\pi(\mathbf{x}_0) \propto q(\mathbf{x}_0; \beta)p_\theta(\mathbf{x}_0)$ amounts to sampling $\mathbf{x}_0$ according to Equation 8, and using some form of MCMC-type sampling with annealing for β to target Equation 3. In cases where f is non-convex and/or induces a highly rugged loss landscape, making sampling either highly inefficient or challenging to tune (Kong et al., 2024).

Instead, we consider using the intermediate unconditional transition functions of the diffusion model, $p_\theta(\mathbf{x}_t \mid \mathbf{x}_{t+1})$, and guide these with the objective function. Using some annealing schedule, $\gamma(t)$, we construct a sequence $\{q_t(\mathbf{x}_t; \gamma_t)\}_{t=0}^T$. Loosely (though concretely in Section 3.2), we may view q_t as a likelihood, with f emitting observations $\mathbf{y}_t$ based on $\mathbf{x}_t$. That is, we may consider $q_t(\mathbf{x_t}; \gamma_t)$ as some $g(\mathbf{y}_t \mid \mathbf{x}_t)$. The task is now frameable through a Bayesian filtering lens, with the intermediate targets being

$$p(\mathbf{x}_t \mid \mathbf{y}_{T:t}) \propto p(\mathbf{x}_t \mid \mathbf{y}_{T:t+1})g(\mathbf{y}_t \mid \mathbf{x}_t) \tag{17}$$

(as in Equation 14 with time reversed). SMC methods provide a principled method of targeting these and ultimately $p(\mathbf{x}_0 \mid \mathbf{y}_{0:T}) \approx q_\infty \propto q(\mathbf{x}; \infty)p_\theta(\mathbf{x})$ of Proposition 2.2.1, yielding $\{\mathbf{x}_i^*\}_{i=1}^M$.

Remark 3.1.1 (Diffusion Models Learn Data Manifolds)**.** A key feature which enables p_θ to act as a good prior is the ability of diffusion models to implicitly learn the data manifold (De Bortoli et al., 2021; Pidstrigach, 2022; Wenliang & Moran, 2023). In the context of optimization, the diffusion model essentially enables us to only consider optimization over 'sensible' values of $\mathbf{x}$; a feasibility constraint. Put differently, the unconditional diffusion prior acts as a regularization to encourage optimization of f over $\mathcal{X} \subseteq \mathbb{R}^{d_x}$ as opposed to over all of $\mathbb{R}^{d_x}$ (Guo et al., 2024).

If we consider the *bootstrap* proposal, $r(\cdot \mid \mathbf{x}_{t+1}, \mathbf{y}) = p_\theta(\cdot \mid \mathbf{x}_{t+1})$, then the weight function in Equation 15 reduces to $g(\mathbf{y}_t \mid \mathbf{x}_t) = q_t(\mathbf{x}; \gamma_t)$, the 'likelihood'. In the case where $q_t(\mathbf{x}_t; \gamma_t)$ is 'peaky' over its support (which is guaranteed for t close to 0 assuming reasonable annealing), this will generally be a poor proposal (Chopin & Papaspiliopoulos, 2020), as its akin to the 'observations', $\mathbf{y}_t$, being informative about the 'states', $\mathbf{x}_t$. The obvious remedy is to choose a better proposal. In the case of general optimization, however, this is a non-trivial task.

Instead we consider using an *auxiliary variable*, adjusting the weight for each particle based on their *previous* likelihood. Heuristically, this implies we weight more heavily those particles whose likelihood *significantly increased* compared to their previous position. This imposes a form of regularization that implicitly discourages concentration on high likelihood regions near the initial distribution, $p(\mathbf{x}_T)$. Geometrically, this regularization may be viewed as dynamically flattening the optimization landscape for each particle based on its position. The role of $\gamma(t)$ is to provide global annealing of the landscape, gradually attenuating this dynamic effect and ultimately applying Proposition 2.2.1 to enable sampling from Q_∞. The full algorithm is described in Algorithm 1.

Remark 3.1.2 (Auxiliary Variable)**.** The concept of using an auxiliary variable to adjust the weights is the foundation of the *auxiliary particle filter* (Chopin & Papaspiliopoulos,

Algorithm 1 `SMCDiffOpt` for General Optimization

Require: $f : \mathcal{X} \to \mathbb{R}$, an objective function to *minimize* (take $-f$ to *maximize*).
Require: $s_\theta(\mathbf{x}_t, t)$, a pre-trained score network (or noise-predictor and apply Proposition 2.3.1).
Require: $r(\cdot \mid \mathbf{x}_{t+1})$, a proposal distribution. Default to $p_\theta(\cdot \mid \mathbf{x}_{t+1})$.
Require: $\gamma(t)$, some annealing schedule.
Require: N, number of particles to use.
  Draw $\mathbf{x}_T^{(i)} \sim \mathcal{N}(0, \mathbf{I}_{d_x}), \quad i = 1, \ldots, N$
  for $t \leftarrow T-1$ to 0 **do**
    for $i \leftarrow 1$ to N **do**
      Move: $\tilde{\mathbf{x}}_t^{(i)} \sim r(\cdot \mid \mathbf{x}_{t+1})$
      Compute weight:

$$\omega_t^{(i)} \leftarrow \frac{\exp\left\{-\gamma(t) f(\tilde{\mathbf{x}}_t^{(i)})\right\}}{\exp\left\{-\gamma(t+1) f(\mathbf{x}_{t+1}^{(i)})\right\}} \tag{18}$$

      Normalise weight: $W_t^{(i)} \leftarrow \frac{\omega_t^{(i)}}{\sum_{i=1}^N \omega_t^{(i)}}$
      Resample: $\{\mathbf{x}_{T:t}^{(i)}\}_{i=1}^N \sim \text{Multinomial}\left(\{\tilde{\mathbf{x}}_{T:t}^{(i)}\}_{i=1}^N; \{W_t^{(i)}\}_{i=1}^N\right)$
    end for
  end for
  return $\{\mathbf{x}_0^{(i)}\}_{i=1}^N$, some summary statistic computed using $\{w_0^{(i)}\}_{i=1}^N$, or some $\{\mathbf{x}_0^{(i)}\}_{i \in \mathcal{I}}$ subset which achieve the (perhaps within a threshold) minimal value amongst all particles.

2020) and can be justified analytically. The exact procedure for auxiliary particle filters differs very slightly from that described in Definition 2.4.3, mainly pertaining to the order of operations and how the intermediate distributions are approximated from the particles.

Remark 3.1.3 (Gradient-free)**.** Note that we don't require any gradient information about f. This makes Algorithm 1 suitable in black-box optimization settings where we might only be able to evaluate f and can't access its gradient (by back-propagation or analytically). However, where we can compute the gradient, $\nabla_{\mathbf{x}_t} f(\mathbf{x}_t)$, we can instead consider using these gradients to 'twist' (Wu et al., 2023) the proposal distribution, yielding a proposal $r_t(\cdot \mid \mathbf{x}_{t+1})$ closer to the true 'posterior', $p(\cdot \mid \mathbf{x}_{t+1}, \mathbf{y}_t)$, reducing the variance of the weights and making the sampler more efficient (enabling lower number

of particles, N). We discuss alternative proposals in more detail in Section 3.3, though these typically are only applicable in inverse problem settings. Alternatively, we may consider adding additional steps after moving the particles, nudging (perhaps a subset of) the particles as in Akyildiz and Míguez (2020). Note here though that even with access to gradients, the algorithm offers substantial advantages over standard gradient-based optimization in cases where f is 'peaky'. We demonstrate this experimentally in Section 4.2.

Remark 3.1.4 (Annealing-only)**.** In principle we could remove the auxiliary variable, and just tune the $\gamma(t)$ annealing schedule. In practice, however, this is extremely challenging and adds even heavier dependence on the nature of f; in cases where it's very 'peaky', the annealing schedule needs to be unreasonably gentle (very slowly increasing from 0), which is often infeasible due to the fixed T time-steps that the diffusion sampler takes (would need to consider intermediate diffusions with, for example, extra Langevin steps in a fashion like Janati et al. (2024) to work around). The auxiliary variable helps make the tuning of $\gamma(t)$ much easier by mitigating its importance in adequately flattening the landscape. This was observed strongly in Section 4.2, for example.

Remark 3.1.5 (Adaptive Resampling (Chopin & Papaspiliopoulos, 2020))**.** In practice, we don't usually resample at every iteration in Algorithm 1, instead resampling only when particle diversity falls below some certain threshold (typically using effective sample size as a metric). Given this, the weight formula in Equation 18 is adjusted by pre-multiplying by the previous un-normalised weight (or 1 if resampled); the procedure is otherwise identical.

3.2. Inverse Problems as a Special Case

Proposition 3.2.1 (Obvservation Generation)**.** Let $\mathbf{y} = \mathbf{y}_0 = A\mathbf{x}_0 + \sigma_y \epsilon$ be some noisy linear measurement we have about a desired sample, $\mathbf{x}_0$. Construct a sequence $\{\mathbf{y}_t\}_{t=1}^T$

by $\mathbf{y}_t = a_t \cdot \mathbf{y}_{t-1}$ with a_t of Definition 2.3.2. It follows that:

$$\mathbf{y}_t = c_t \cdot \mathbf{y} \tag{19}$$

From which we may conclude

$$\mathbf{Y}_t \mid \mathbf{X}_0 = \mathbf{x}_0 \sim \mathcal{N}(c_t \cdot A\mathbf{x}_0, c_t^2\sigma_y^2 \cdot \mathbf{I}_{d_y})$$

and

$$\mathbf{Y}_t \mid \mathbf{X}_t = \mathbf{x}_t \sim \mathcal{N}(c_t \cdot A\mathbf{x}_0, c_t^2\sigma_y^2 \cdot \mathbf{I}_{d_y} + d_t^2 \cdot AA^\top) \tag{20}$$

with $g(\mathbf{y}_0 \mid \mathbf{x}_0) = g(\mathbf{y} \mid \mathbf{x}_0) = \mathcal{N}(\mathbf{y}; A\mathbf{x}_0, \sigma_y^2 \cdot \mathbf{I}_{d_y})$ exactly the measurement density.

Proof. See Appendix. □

Remark 3.2.1 (Shrinking)**.** The important characteristic of Equation 19 is that it 'shrinks' the observations towards 0 (in tandem, theoretically, with how $\mathbf{x}_0$ is shrunk towards zero according to its forward process). This essentially creates an *aligned* observation sequence so that the likelihoods (i.e. density evaluations of Equation 20) are sensibly sized, enabling their usage in SMC algorithms.

Importantly, note that this generation does not depend on the clean sample, $\mathbf{x}_0$. As such, it can be generated prior to running the guided sampling and we may view sampling from $p(\mathbf{x}_0 \mid \mathbf{y})$ as a Bayesian filtering task. This is described succinctly in Dou and Song (2023):

> We can generate a sample $\mathbf{x}_0$ from the Bayesian posterior distribution $p_\theta(\mathbf{x}_0 \mid \mathbf{y}_0)$ by first sampling from $p_\theta(\mathbf{y}_{1:T} \mid \mathbf{y}_0)$ before sampling from $p_\theta(\mathbf{x}_0 \mid \mathbf{y}_{0:T})$. This is because $p_\theta(\mathbf{x}_0 \mid \mathbf{y}_0) = \int p_\theta(\mathbf{x}_0 \mid \mathbf{y}_{0:T}) p_\theta(\mathbf{y}_{1:T} \mid \mathbf{y}_0)\, d\mathbf{y}_{1:T}$.

Proposition 3.2.2 (Inverse Problem Objective)**.** Consider the following objective function:

$$f(\mathbf{x}_t) = -\frac{1}{2\sigma_y^2 c_t^2}\|\mathbf{y}_t - A\mathbf{x}_t\|^2 \tag{21}$$

with $\mathbf{y}_t$ constructed from $\mathbf{y}$ according to Equation 19. Plugging this in to Equation 18, ignoring particle indices, the weight function reduces to:

$$\omega_t \leftarrow \frac{\mathcal{N}(\mathbf{y}_t; A\tilde{\mathbf{x}}_t, c_t^2\sigma_y^2 \cdot \mathbf{I}_{d_y} + d_t^2 \cdot AA^\top)^{\gamma(t)}}{\mathcal{N}(\mathbf{y}_{t+1}; A\mathbf{x}_{t+1}, c_{t+1}^2\sigma_y^2 \cdot \mathbf{I}_{d_y} + d_{t+1}^2 \cdot AA^\top)^{\gamma(t+1)}} \tag{22}$$

We see this is exactly the ratio of the likelihoods, annealed according to $\gamma(t)$. Its interpretation is exactly as in Section 3.1 except the notion of observations and posterior densities is now exact.

Remark 3.2.2 (MAP)**.** The choice of f in Equation 21 essentially states that we're choosing to maximize the likelihood, $g(\mathbf{y}_t \mid \mathbf{x}_t)$, subject to the constraint/regularisation imposed by the prior diffusion model through $p_\theta(\cdot \mid \mathbf{x}_{t+1})$. Based on 2.4.3, it follows that running Algorithm 1 seeks ultimately to yield those samples $\{\mathbf{x}_0^{(i)}\}_{i=1}^N$ which are the *maximum a posteriori* estimates of $\mathbf{x}_0$, exactly as desired for solving an inverse problem.

Remark 3.2.3 (Inner Tempering)**.** By symmetry of the Gaussian distribution, we have

$$\begin{aligned}\mathcal{N}(\mathbf{y}_t; A\mathbf{x}_t, c_t^2\sigma_y^2 \cdot \mathbf{I}_{d_y} + d_t^2 \cdot AA^\top) &= \mathcal{N}(A\mathbf{x}_t; \mathbf{y}_t, c_t^2\sigma_y^2 \cdot \mathbf{I}_{d_y} + d_t^2 \cdot AA^\top) \\ &= \mathcal{N}(A\mathbf{x}_t; c_t\mathbf{y}, c_t^2\sigma_y^2 \cdot \mathbf{I}_{d_y} + d_t^2 \cdot AA^\top)\end{aligned}$$

We see that there is essentially an inner-level of tempering according to $c(t)$, defined by the unconditional diffusion model. As such, for inverse problems we can generally take $\gamma(t) = 1\,\forall t$.

Remark 3.2.4 (Non-Linear Case)**. TODO**

3.3. Relation to Related Work

Taking $\mu_{t+1}(\mathbf{x}_{t+1}, \theta), \Sigma_{t+1}$ as the mean (e.g. Equation 9) and variance (e.g. Equation 10) of the backwards transition kernel, $p_\theta(\mathbf{x}_t \mid \mathbf{x}_{t+1})$, and Ξ_t as the covariance of 20 the Monte Carlo Guided Diffusion (MCGdiff) (Cardoso et al., 2023) and Filter Posterior Sampling SMC (FPS-SMC) (Dou & Song, 2023) frameworks consider essentially equivalent proposals:

$$r(\tilde{\mathbf{x}}_t \mid \mathbf{x}_{t+1}, \mathbf{y}_t) \propto p_\theta(\tilde{\mathbf{x}}_t \mid \mathbf{x}_{t+1}) g(\mathbf{y}_t \mid \tilde{\mathbf{x}}_t) = \mathcal{N}(\mu^*_{t+1}(\mathbf{x}_{t+1}, \mathbf{y}_t, \theta), \Sigma^*_{t+1})$$

(by Normal-Normal conjugacy) with

$$\begin{aligned} \Sigma^*_{t+1} &= \left(\Sigma^{-1}_{t+1} + A^\top \Xi^{-1} A\right)^{-1} \\ \mu^*_{t+1}(\mathbf{x}_{t+1}, \mathbf{y}_t, \theta) &= \Sigma^*_{t+1} \cdot \left(\Sigma^{-1}_{t+1} \mu_{t+1}(\mathbf{x}_{t+1}, \theta) + A^\top \Xi^{-1} \mathbf{y}_t\right) \end{aligned}$$

and $\mathbf{y}_t$ constructed by Equation 19[1] and g as in Equation 20. Plugging this in to Equation 15, we get:

$$\begin{aligned} \omega_t &= \int p_\theta(\tilde{\mathbf{x}}_t \mid \mathbf{x}_{t+1}) g(\mathbf{y}_t \mid \tilde{\mathbf{x}}_t)\, d\mathbf{x}_t = g(\mathbf{y}_t \mid \mathbf{x}_{t+1}) \\ &= \mathcal{N}\left(\mathbf{y}_t; A\mu_{t+1}(\mathbf{x}_{t+1}, \theta), \Xi_t + A\Sigma_{t+1}A^\top\right) \end{aligned}$$

where we apply Proposition B.1. Note this *only* holds when we have a linear inverse problem; otherwise $g(\mathbf{y}_t \mid \mathbf{x}_{t+1})$ is intractable. In the case of FPS-SMC, these are exactly the weights used in the SMC procedure; in the case of MCGDiff they similarly use the previous likelihood, $g(\mathbf{y}_{t+1} \mid \mathbf{x}_{t+1})$, as an auxiliary variable. Through this lens, we may view MCGDiff as a special case of Algorithm 1 where we choose:

$$f(\tilde{\mathbf{x}}_t) = g(\mathbf{y}_t \mid \mathbf{x}_{t+1}) = \mathcal{N}\left(\mathbf{y}_t; A\mu_{t+1}(\mathbf{x}_{t+1}, \theta), \Xi_t + A\Sigma_{t+1}A^\top\right)$$

[1] Dou and Song (2023) considers a slightly different construction which employs "noise-sharing" with the state's forward-process; see D.

but keep the auxiliary variable (abusing notation) as $f(\mathbf{x}_{t+1}) = g(\mathbf{y}_{t+1} \mid \mathbf{x}_{t+1})$. The interpretation is very similar to before except rather than more strongly weighting those particles whose likelihood *increased* relative to their previous position, we more strongly weight those whose whose likelihood *will increase with the next transition* relative to their previous position more strongly. The idea is then to properly implement an auxiliary particle filter, and weight particles *before* moving them. This generally should improve the performance since it's essentially 'forward-looking'. However, it's important to note this can only be applied to *linear inverse problems* due to the intractability of $g(\mathbf{y}_t \mid \mathbf{x}_{t+1})$ generally; it similarly cannot be applied for general optimization tasks.

With that said, there is nothing prohibiting us from using other proposals, such as that of MCGDiff/FPS-SMC, in Algorithm 1, re-deriving the weight function for Equation 22 from Equation 15 but still using the previous likelihood auxiliary variable. As mentioned in Remark 3.1.3, we could consider using gradients to construct the proposals. Wu et al. (2023) consider $\nabla_{\mathbf{x}_t} \log p_{\mathbf{y}|\hat{\mathbf{x}}_0(\mathbf{x}_t,\theta)}$ (with $\hat{\mathbf{x}}_0(\mathbf{x}_t, \theta)$ as in Equation 5) computed using back-propagation through the network, s_θ, to twist the proposal. Boys et al. (2023) consider $\nabla_{\mathbf{x}_t}\hat{\mathbf{x}}_0(\mathbf{x}_t, \theta)$ to choose a more optimal covariances in $p_\theta(\mathbf{x}_{t-1} \mid \mathbf{x}_t)$. Such methods incur additional computational cost and are, again, restricted to linear inverse problems. In such cases, however, the added efficiency of the proposal can (significantly) reduce the number of particles, N, mitigating some of this added computational cost.

TODO: Move some of related work/alternative methods at end of 4 to here; include Guo et al., 2024 and Kong et al., 2024.

4. Experiments and Results

4.1. Gaussian Mixture Model Inverse Problem Experiment

Beginning with an inverse problem, we consider the synthetic experiment described in Boys et al. (2023) and Cardoso et al. (2023). Consider a Gaussian mixture model (GMM), p_{data}, with 25 equally weighted ($\omega_{i,j} \propto 1$) d_x-dimensional Gaussian random variables with means $\mu_{i,j} := (8i, 8j, \ldots, 8i, 8j) \in \mathbb{R}^{d_x}$ for $(i, j) \in \{-2, \ldots, 2\}^2$ and unit variance. We generate some d_y-dimensional measurement, $\mathbf{y}$, according to the following process:

- Draw $\tilde{A} \sim \mathcal{N}(0, 1)^{d_y \times d_x} \in \mathbb{R}^{d_y \times d_x}$ and compute its SVD decomposition, $USV^\top$.
- Sample $s_{i,j} \sim \mathcal{U}[0, 1]$ for $(i, j) \in \{-2, \ldots, 2\}^2$.
- Set $A := U\, diag(\{s_{i,j}\})\, V^\top$.
- Draw $\mathbf{x}_* \sim p_{\text{data}}$ and set $\mathbf{y} := A\mathbf{x}_* + \sigma_y \epsilon,\ \epsilon \sim \mathcal{N}(\mathbf{0}_{d_y}, \mathrm{I}_{d_y})$

The goal of the inverse problem is to take $\mathbf{y}$ (with A and σ_y known), and use it to infer $\mathbf{x}_*$. We consider $d_y < d_x$, making the problem ill-posed. Per Remark 2.1.1, we tackle this by considering $p_{\text{data}}(\mathbf{x})$ as a prior distribution, $g(\mathbf{y} \mid \mathbf{x}) = \mathcal{N}(\mathbf{y}; A\mathbf{x}, \sigma_y \mathbf{I}_{d_y})$ as the measurement density, and then aim to sample from $p(\mathbf{x} \mid \mathbf{y})$.

d_x	d_y	SMCDiffOpt	DPS	IIIGD	TMPD
8	1	1.35 ± 1.0	8.18 ± 7.5	3.16 ± 2.72	3.31 ± 2.86
	2	0.55 ± 0.43	2.72 ± 2.62	0.94 ± 0.89	1.34 ± 1.25
	4	0.19 ± 0.09	0.95 ± 0.9	0.09 ± 0.03	0.37 ± 0.33
80	1	1.65 ± 1.41	5.03 ± 4.63	3.08 ± 2.71	2.42 ± 1.71
	2	1.19 ± 1.07	3.14 ± 3.02	1.68 ± 1.62	1.35 ± 1.22
	4	1.11 ± 0.93	1.32 ± 1.21	0.84 ± 0.79	1.14 ± 0.9

Table 4.1.: Sliced-Wasserstein distances of samples from particle samples.

For this model, given p_{data} is available in closed form, the posterior, $p(\mathbf{x}_* \mid \mathbf{y})$, is actually available in closed form as another GMM with:

$$c_{i,j} := \mathcal{N}\left(\Sigma\left(\sigma_y^{-2} \cdot A^\top \mathbf{y} + \mu_{i,j}\right), \Sigma\right)$$
$$\tilde{\omega}_{i,j} \propto \omega_{i,j} \mathcal{N}\left(\mathbf{y}; A\mu_{i,j}, \mathbf{I}_{d_x} + AA^\top\right)$$

with $\Sigma := \left(\mathbf{I}_{d_x} + \sigma_y^{-2} \cdot A^\top A\right)^{-1}$. This enables us to accurately benchmark the different numerical methods.

Supposing p_{data} was not available in closed form / easy to sample from, we may consider using a diffusion model to sample from it. As p_{data} is a GMM, the backwards marginal is also available in closed form allowing us to avoid training a score network, being able to use simple auto-differentiation of the marginal to yield the exact score at intermediate time-steps in a diffusion process. Then using Equation 4, we can sample from p_{data} in some T time-steps. We can then apply our method, as described in Section 3.2 with $\gamma(t) = 1$, to guide the process to enable sampling from the posterior, $p(\mathbf{x} \mid \mathbf{y})$. We can contrast this with the non-particle based approaches of Boys et al. (2023), Chung et al. (2022), and J. Song et al. (2023) [1], using sliced-Wasserstein distance (Boys et al., 2023; Cardoso et al., 2023) to measure how well each method approximates the true posterior distribution based on samples drawn directly from it.

We experiment for $d_x \in \{8, 80\}$, $d_y \in \{1, 2, 4\}$, and $\sigma_y \in \{0.01, 0.1, 1.0\}$, comparing the performance of `SMCDiffOpt`, diffusion-posterior-sampling (DPS; Chung et al., 2022),

[1] See Section C for discussion as why MCGdiff comparison was excluded.

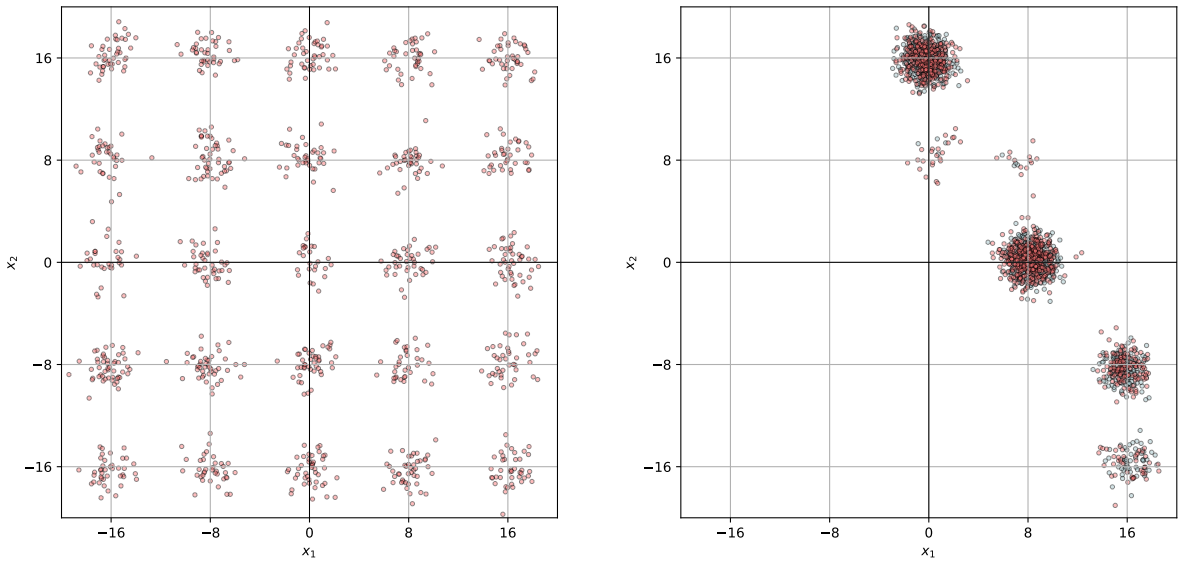

(a) Prior samples generated under DDPM with analytic score.

(b) `SMCDiffOpt` samples for a particular measurement model; $d_x = 8, d_y = 2$.

Figure 4.1.: Prior versus posterior samples under guidance through `SMCDiffOpt`.

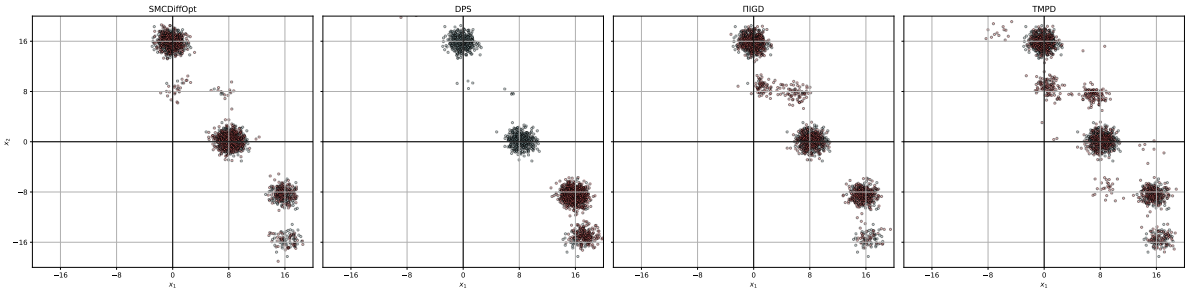

Figure 4.2.: Comparison of samples against true posterior samples; $d_x = 8; d_y = 2$.

pseudo-inverse-guided-diffusion (ΠIGD; J. Song et al., 2023), and Tweedie-moment-projected-diffusion (TMPD; Boys et al., 2023). We run the experiment for 10 different seeds, generating 10 different measurement models according to the above steps, using 1000 particles for `SMCDiffOpt` and generating 1000 independent samples for the other methods, all in 1000 time-steps under DDPM sampling.

The results are shown in Table 4.1 rolled up on σ_y; in Table A.1 we show the full-results split out by σ_y[2]. The values shown are the median and ranges for the sliced-Wasserstein distance over the seeds. We see that `SMCDiffOpt` outperforms the other methods. In

[2]This table roughly aligns with Table 4 of Boys et al. (2023), providing some level of validation.

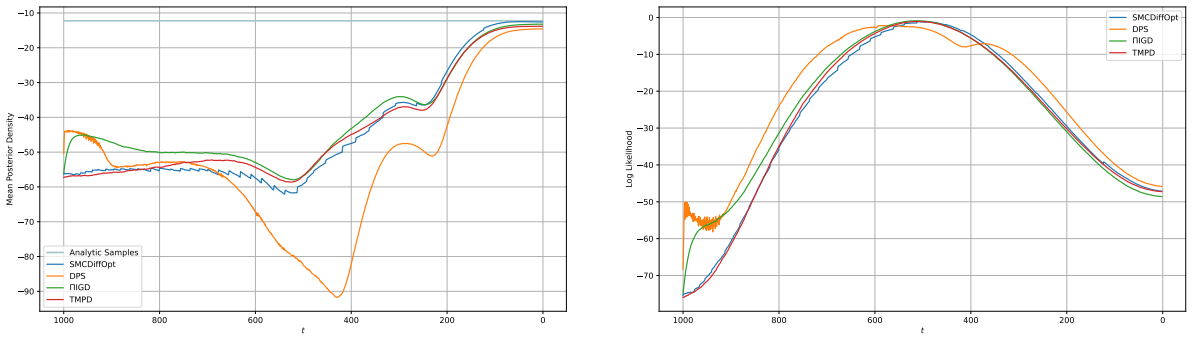

(a) Log-Posterior density over time.

(b) Log-Likelihood over time.

Figure 4.3.: Mean log-posterior and log-likelihood of samples over time with respect to observations, $\{\mathbf{y}_t\}_{t=1}^T$, constructed per Equation 19; associated with Figure 4.2.

Figure 4.2 we plot the first two co-ordinates of the samples generated by each method overlaying true posterior samples for a specific measurement model with $d_x = 8, d_y = 2$, providing visual confirmation.

In Figure 4.3 we show the evolution of the true (log) posterior density evaluated on the sample at step t, $p_{\mathbf{x}_0|\mathbf{y}}(\mathbf{x}_t \mid \mathbf{y})$, and (log) likelihood, $g(\mathbf{y}_t \mid \mathbf{x}_t)$, over the course of the guided diffusions under each method. Figure 4.3a shows how well the methods ultimately target the posterior distribution; we see that all but DPS track follow similar trajectories. Examining Figure 4.3b in conjunction, we see that the methods appear to operate by first optimizing the likelihood to a point before turning to optimize the posterior density, allowing the likelihood to decline. Essentially, Figure 4.3 highlights the regularization effect of the diffusion prior model.

Note that the numeric comparison of `SMCDiffOpt` with the other three methods isn't entirely fair since the former is an interacting-particle algorithm; `SMCDiffOpt` requires several particles to operates whereas the others are independent runs. Reducing the number of particles will almost definitionally reduce the relative outperformance of `SMCDiffOpt` over the others. However, we might reasonably infer from these results that `SMCDiffOpt` will likewise perform well on general (non-linear) inverse problems, where ΠIGD and TMPD can't be used, given Algorithm 1 only relied on access to the likelihood function and the transition function while still being able to well-target the posterior.

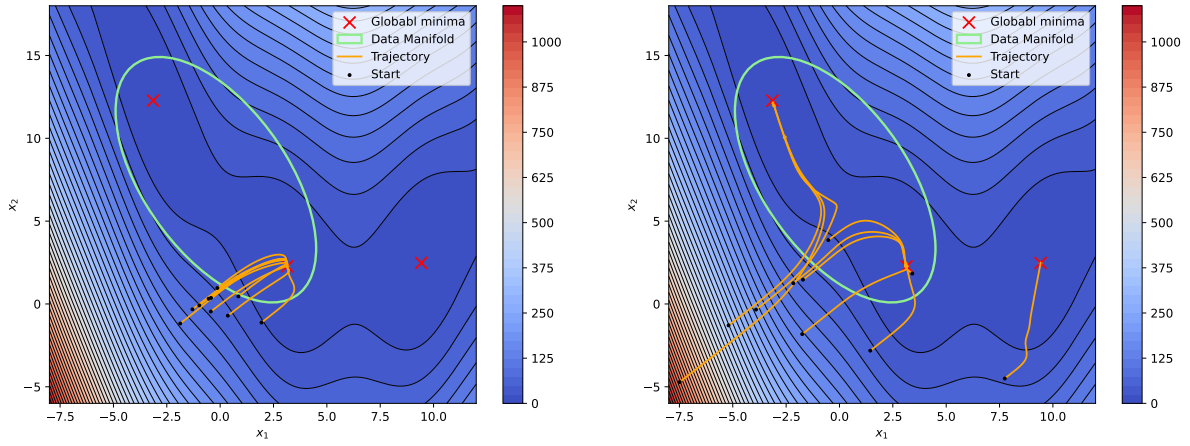

(a) Adam with $\mathcal{N}(0, \mathbf{I}_{d_x})$ initialisation.

(b) Adam with $\mathcal{N}(0, 16 \cdot \mathbf{I}_{d_x})$ initialisation.

Figure 4.4.: Pitfalls of naieve gradient optimisation of the Branin function.

4.2. Branin Function Optimization Experiment

For a general optimization task, we consider optimizing the Branin function as an objective over some constrained region (the data manifold) as detailed in Kong et al. (2024). The Branin function is defined by:

$$f(x_1, x_2) = a(x_2 - bx_1^2 + cx_1 - r)^2 + s(1-t)\cos(x_1) + s \tag{23}$$

where $a = 1$, $b = \frac{5.1}{4\pi^2}$, $c = \frac{5}{\pi}$, $r = 6$, $s = 10$, $t = \frac{1}{8\pi}$. It has three global minimas located at $(-\pi, 12.275)$, $(\pi, 2.275)$ and $(9.42478, 2.475)$, with a value of 0.397887. We consider some uniform prior sampling distribution, p_{data}, over an ellipse region centered at $(-0.2, 7.5)$ with semi-axis lengths $(3.6, 8)$, tilted 25°. This region covers two of the global minima $(-\pi, 12.275)$ and $(\pi, 2.275)$. See Figure 4.4 to visualize.

Similar to in Section 4.1, here we can easily sample from p_{data} by inverse-transform sampling. Again, we suppose now that we can't do so and suppose also that we're in a high-dimensional setting where performing a simple visual analysis to quickly infer the geometry of the objective function and data manifold is not possible. Our stated objective is to optimize the function over the data manifold, ideally finding the $(-\pi, 12.275)$ and $(\pi, 2.275)$ points, but *not* the $(9.42478, 2.475)$ point (since it's outside the con-

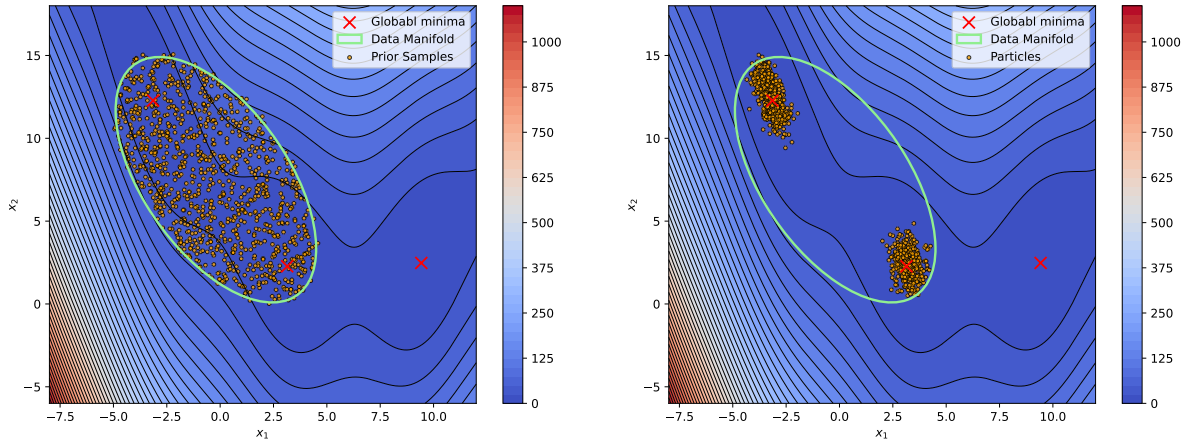

(a) Prior samples from trained model well-targetting the data manifold.

(b) `SMCDiffOpt`'s resulting particles from optimizing the Branin function.

Figure 4.5.: Prior versus optimised samples under guidance through `SMCDiffOpt`.

strained region / not a *valid configuration*).

The obvious approach might be to use a gradient-based optimizer, such as the popular Adam (Kingma & Ba, 2017), adaptive-moment-estimating optimizer. However, without prior knowledge of the data manifold, choosing initial points for the optimizer is challenging. In Figure 4.4a we show choosing 10 (for visual clarity) starting points randomly from a $\mathcal{N}(0, \mathbf{I}_{d_x})$ distribution. Using a base learning rate of 0.05 and 1000 iterations of the optimizer, we see that in this case the optimizer does find one of the optima, but has essentially no chance of finding the other. In Figure 4.4b we re-run the optimizer but with initial points randomly from a $\mathcal{N}(0, 16 \cdot \mathbf{I}_{d_x})$ distribution instead. Here we see that while the optimizer found the two desired points, it also found one of the points outside the constrained region — an invalid configuration. Furthermore, we see that one of trajectories didn't converge to an optima; this sample headed towards the saddle-point region between the two optima and essentially got stuck there requiring many iterations to escape. The key issue here is that the optimizer has no guidance towards the data manifold and relies solely on the gradient. Obviously, if we could sample from p_{data} analytically, choosing this as the distribution to pick initial samples is optimal. Since we can't generally, we resort to generative techniques, such as diffusion models.

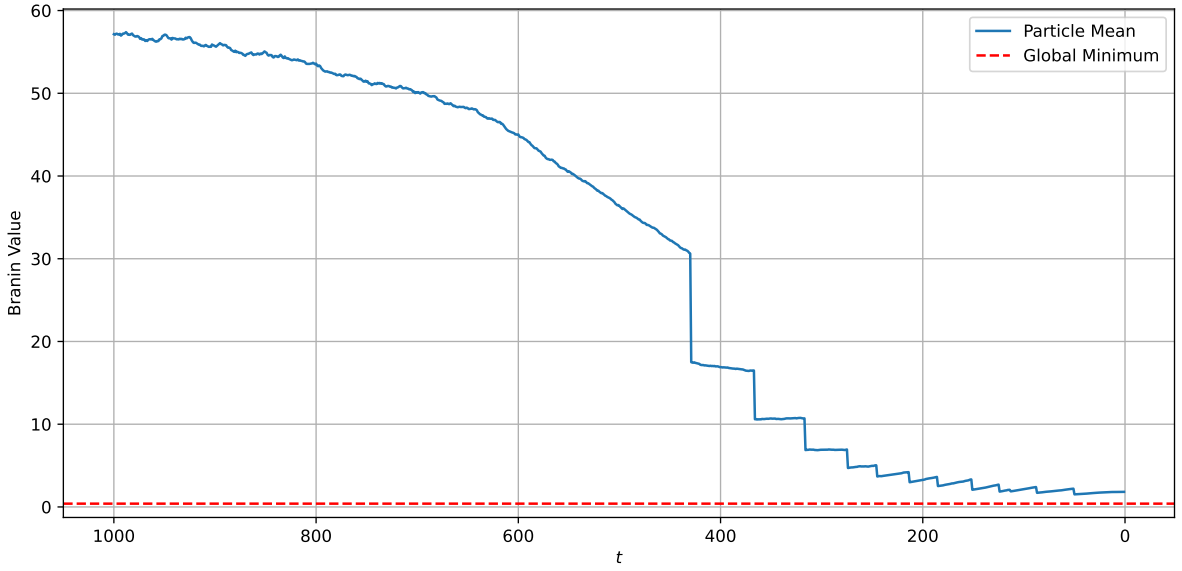

Figure 4.6.: Mean value of Equation 23 on particles over time.

To apply `SMCDiffOpt`, we sample training data from p_{data}[3], and use this to train a simple score-based diffusion model (details in Section C). With such a model, we can now approximately generate samples from p_{data}. More importantly, we can use the model as a prior, using it as transition kernel in Algorithm 1, with the 'likelihood' being an (annealed) induced Boltzmann distribution from the Branin function. Choosing $\gamma(t) = 1 - e^{-\zeta T}$ for some small, tunable ζ (e.g. 0.001), we run Algorithm 1 with 1000 particles. In Figure 4.5b, we see that the procedure has well-discovered the two desired optima; using the final particle weights the precise global minima can be easily discovered. This is further highlighted in Figure 4.6.

The remarkable feature of Algorithm 1 is that it can achieve this optimisation without requiring access to the gradient of the objective. As mentioned in Chapter 3, if we did have access to these gradients we could consider using them with Algorithm 1 either as an additional step after moving the particles ("gradient nudging"; (Akyildiz & Míguez, 2020)) or as a means of picking a better proposal distribution ("twisting"; (Wu et al., 2023)). In such cases, the requisite number of particles and the reliance on the $\gamma(t)$

[3]Obviously, we are supposing this sampling isn't generally possible; we are in a generative modelling situation where we pre-suppose access to a finite number of samples from p_{data} a priori, and train a model on these, hoping it enables general sampling from p_{data}.

schedule should likely reduce. A completely alternative approach might be that of Kong et al. (2024) who consider guiding the diffusion directly with an annealed gradient and then running some Langevin steps (i.e. MALA) after. This can work well but has the downside of relying on the gradient which means its usage in black-box settings requires the training of a surrogate model.

4.3. Black-Box Optimization Experiment

TODO

5. Discussion

TODO; appx 1.5 pages

- Re-describe benefits of approach and relative contribution of work.
- Re-describe limitations/shortcomings of approach.
- Discuss future work; ablation study, incorporation of gradients, non-linear inverse problems, apply to imagery or other high-dim inverse problems, full black-box benchmark
- Summary concluding remarks.

6. Endmatter

All code for the research is openly available on a GitHub repository. All results in this paper can be easily reproduced by following the instructions of said repository's `README`. Code was run on an NVIDIA RTX3080.

Black-box data and oracle models are available originally through the `design-bench` repository.

References

Akyildiz, Ö. D., & Míguez, J. (2020). Nudging the particle filter. *Statistics and Computing*, *30*(2), 305–330. https://doi.org/10.1007/s11222-019-09884-y

Anderson, B. D. (1982). Reverse-time diffusion equation models. *Stochastic Processes and their Applications*, *12*(3), 313–326. https://doi.org/10.1016/0304-4149(82)90051-5

Boys, B., Girolami, M., Pidstrigach, J., Reich, S., Mosca, A., & Akyildiz, O. D. (2023, November 22). *Tweedie Moment Projected Diffusions For Inverse Problems*. arXiv: 2310.06721 [stat]. Retrieved June 23, 2024, from http://arxiv.org/abs/2310.06721

Cardoso, G., Idrissi, Y. J. E., Corff, S. L., & Moulines, E. (2023, October 25). *Monte Carlo guided Diffusion for Bayesian linear inverse problems*. arXiv: 2308.07983 [cs, stat]. https://doi.org/10.48550/arXiv.2308.07983

Chopin, N., & Papaspiliopoulos, O. (2020). *An introduction to sequential Monte Carlo*. Springer.

Chung, H., Kim, J., Mccann, M. T., Klasky, M. L., & Ye, J. C. (2022). Diffusion Posterior Sampling for General Noisy Inverse Problems. https://doi.org/10.48550/ARXIV.2209.14687

De Bortoli, V., Thornton, J., Heng, J., & Doucet, A. (2021, June 1). *Diffusion Schr\"odinger Bridge with Applications to Score-Based Generative Modeling*. arXiv.org. Retrieved August 19, 2024, from https://arxiv.org/abs/2106.01357v5

Del Moral, P. (2011). Central Limit Theorems. In *Feynman-Kac formulae: Genealogical and interacting particle systems with applications* (pp. 291–330). Springer. OCLC: 1063493341.

Dhariwal, P., & Nichol, A. (2021, June 1). *Diffusion Models Beat GANs on Image Synthesis*. arXiv: 2105.05233 [cs, stat]. https://doi.org/10.48550/arXiv.2105.05233

Dou, Z., & Song, Y. (2023). Diffusion Posterior Sampling for Linear Inverse Problem Solving: A Filtering Perspective. Retrieved June 8, 2024, from https://openreview.net/forum?id=tplXNcHZs1&referrer=%5Bthe%20profile%20of%20Yang%20Song%5D(%2Fprofile%3Fid%3D~Yang_Song1)

Guo, Y., Yuan, H., Yang, Y., Chen, M., & Wang, M. (2024, April 23). *Gradient Guidance for Diffusion Models: An Optimization Perspective*. arXiv: 2404.14743 [cs, stat]. Retrieved July 26, 2024, from http://arxiv.org/abs/2404.14743

Ho, J., Jain, A., & Abbeel, P. (2020). Denoising Diffusion Probabilistic Models. https://doi.org/10.48550/ARXIV.2006.11239

Ho, J., Salimans, T., Gritsenko, A., Chan, W., Norouzi, M., & Fleet, D. J. (2022, June 22). *Video Diffusion Models*. arXiv: 2204.03458 [cs]. Retrieved August 21, 2024, from http://arxiv.org/abs/2204.03458

Hwang, C.-R. (1980). Laplace's Method Revisited: Weak Convergence of Probability Measures. *The Annals of Probability*, *8*(6). https://doi.org/10.1214/aop/1176994579

Janati, Y., Durmus, A., Moulines, E., & Olsson, J. (2024, March 17). *Divide-and-Conquer Posterior Sampling for Denoising Diffusion Priors*. arXiv: 2403.11407 [cs, stat]. Retrieved May 24, 2024, from http://arxiv.org/abs/2403.11407

Kingma, D. P., & Ba, J. (2017, January 29). *Adam: A Method for Stochastic Optimization*. arXiv: 1412.6980 [cs]. https://doi.org/10.48550/arXiv.1412.6980

Kong, L., Du, Y., Mu, W., Neklyudov, K., De Bortoli, V., Wang, H., Wu, D., Ferber, A., Ma, Y.-A., Gomes, C. P., & Zhang, C. (2024, April 29). *Diffusion Models as Constrained Samplers for Optimization with Unknown Constraints*. arXiv: 2402.18012 [cs]. Retrieved July 26, 2024, from http://arxiv.org/abs/2402.18012

Krishnamoorthy, S., Mashkaria, S. M., & Grover, A. (2023, August 21). *Diffusion Models for Black-Box Optimization*. arXiv: 2306.07180 [cs]. Retrieved July 31, 2024, from http://arxiv.org/abs/2306.07180

Li, X., Ren, Y., Jin, X., Lan, C., Wang, X., Zeng, W., Wang, X., & Chen, Z. (2023). Diffusion Models for Image Restoration and Enhancement – A Comprehensive Survey. https://doi.org/10.48550/ARXIV.2308.09388

Nichol, A., & Dhariwal, P. (2021, February 18). *Improved Denoising Diffusion Probabilistic Models*. arXiv: 2102.09672 [cs, stat]. Retrieved May 29, 2024, from http://arxiv.org/abs/2102.09672

Nichol, A., Dhariwal, P., Ramesh, A., Shyam, P., Mishkin, P., McGrew, B., Sutskever, I., & Chen, M. (2021). GLIDE: Towards Photorealistic Image Generation and Editing with Text-Guided Diffusion Models. https://doi.org/10.48550/ARXIV.2112.10741

Pidstrigach, J. (2022). Score-Based Generative Models Detect Manifolds. https://doi.org/10.48550/ARXIV.2206.01018

Rombach, R., Blattmann, A., Lorenz, D., Esser, P., & Ommer, B. (2021). High-Resolution Image Synthesis with Latent Diffusion Models. https://doi.org/10.48550/ARXIV.2112.10752

Saharia, C., Chan, W., Chang, H., Lee, C. A., Ho, J., Salimans, T., Fleet, D. J., & Norouzi, M. (2021). Palette: Image-to-Image Diffusion Models. https://doi.org/10.48550/ARXIV.2111.05826

Saharia, C., Chan, W., Saxena, S., Li, L., Whang, J., Denton, E., Ghasemipour, S. K. S., Ayan, B. K., Mahdavi, S. S., Lopes, R. G., Salimans, T., Ho, J., Fleet, D. J., & Norouzi, M. (2022). Photorealistic Text-to-Image Diffusion Models with Deep Language Understanding. https://doi.org/10.48550/ARXIV.2205.11487

Sohl-Dickstein, J., Weiss, E., Maheswaranathan, N., & Ganguli, S. (2015, July 7–9). Deep unsupervised learning using nonequilibrium thermodynamics. In F. Bach & D. Blei (Eds.), *Proceedings of the 32nd international conference on machine learning* (pp. 2256–2265, Vol. 37). PMLR. https://proceedings.mlr.press/v37/sohl-dickstein15.html

Song, J., Meng, C., & Ermon, S. (2020). Denoising Diffusion Implicit Models. https://doi.org/10.48550/ARXIV.2010.02502

Song, J., Vahdat, A., Mardani, M., & Kautz, J. (2023). Pseudoinverse-guided diffusion models for inverse problems. *International Conference on Learning Representations*. https://openreview.net/forum?id=9_gsMA8MRKQ

Song, Y., & Ermon, S. (2020, October 10). *Generative Modeling by Estimating Gradients of the Data Distribution*. arXiv: 1907.05600 [cs, stat]. https://doi.org/10.48550/arXiv.1907.05600

Song, Y., Sohl-Dickstein, J., Kingma, D. P., Kumar, A., Ermon, S., & Poole, B. (2021, February 10). *Score-Based Generative Modeling through Stochastic Differential Equations*. arXiv: 2011.13456 [cs, stat]. Retrieved May 31, 2024, from http://arxiv.org/abs/2011.13456

Trabucco, B., Geng, X., Kumar, A., & Levine, S. (2022, February 17). *Design-Bench: Benchmarks for Data-Driven Offline Model-Based Optimization*. arXiv: 2202.08450 [cs]. https://doi.org/10.48550/arXiv.2202.08450

Trippe, B. L., Yim, J., Tischer, D., Baker, D., Broderick, T., Barzilay, R., & Jaakkola, T. (2023, March 19). *Diffusion probabilistic modeling of protein backbones in 3D for the motif-scaffolding problem*. arXiv: 2206.04119 [cs, q-bio, stat]. Retrieved June 5, 2024, from http://arxiv.org/abs/2206.04119

Wenliang, L. K., & Moran, B. (2023, November 16). *Score-based generative models learn manifold-like structures with constrained mixing*. arXiv: 2311.09952 [cs, stat]. https://doi.org/10.48550/arXiv.2311.09952

Wu, L., Trippe, B. L., Naesseth, C. A., Blei, D. M., & Cunningham, J. P. (2023, June 30). *Practical and Asymptotically Exact Conditional Sampling in Diffusion Models*. arXiv: 2306.17775 [cs, q-bio, stat]. Retrieved June 5, 2024, from http://arxiv.org/abs/2306.17775

Xu, M., Yu, L., Song, Y., Shi, C., Ermon, S., & Tang, J. (2022, March 6). *GeoDiff: A Geometric Diffusion Model for Molecular Conformation Generation*. arXiv: 2203.02923 [cs, q-bio]. Retrieved August 21, 2024, from http://arxiv.org/abs/2203.02923

Appendices

A. Additional Tables and Figures

σ_y	d_x	d_y	SMCDiffOpt	DPS	ΠGD	TMPD
0.0	8	1	0.98 ± 0.44	8.22 ± 7.32	3.15 ± 2.58	3.5 ± 2.67
		2	0.55 ± 0.43	0.41 ± 0.29	0.33 ± 0.27	0.44 ± 0.34
		4	0.21 ± 0.07	0.12 ± 0.06	0.09 ± 0.03	0.08 ± 0.04
	80	1	0.75 ± 0.31	2.45 ± 1.79	3.18 ± 2.6	2.66 ± 1.47
		2	1.22 ± 1.04	1.35 ± 1.21	0.33 ± 0.27	0.81 ± 0.68
		4	0.26 ± 0.05	0.97 ± 0.86	0.08 ± 0.02	0.68 ± 0.44
0.1	8	1	1.13 ± 0.51	8.18 ± 7.5	3.22 ± 2.67	3.11 ± 2.31
		2	0.2 ± 0.07	0.38 ± 0.28	0.19 ± 0.13	0.43 ± 0.34
		4	0.15 ± 0.05	0.16 ± 0.06	0.07 ± 0.01	0.06 ± 0.01
	80	1	1.25 ± 1.02	2.51 ± 2.11	2.93 ± 2.56	2.56 ± 1.18
		2	0.45 ± 0.32	1.27 ± 1.14	0.62 ± 0.56	0.66 ± 0.54
		4	0.23 ± 0.06	1.03 ± 0.9	0.08 ± 0.02	0.63 ± 0.34
1.0	8	1	1.35 ± 1.0	6.62 ± 4.96	1.16 ± 0.72	1.35 ± 0.9
		2	0.44 ± 0.28	2.92 ± 2.42	0.94 ± 0.89	1.44 ± 1.15
		4	0.15 ± 0.03	1.19 ± 0.66	0.1 ± 0.03	0.45 ± 0.26
	80	1	1.69 ± 1.37	5.26 ± 4.4	1.2 ± 0.79	1.23 ± 0.53
		2	0.89 ± 0.78	3.21 ± 2.95	1.68 ± 1.62	1.41 ± 1.16
		4	1.12 ± 0.92	1.54 ± 0.99	0.89 ± 0.74	1.37 ± 0.67

Table A.1.: Sliced-Wasserstein distances for different σ_y.

B. Proofs

Proof of Proposition 3.2.1. Given:

$$\begin{aligned}
\mathbf{X}_t \mid \mathbf{X}_0 = \mathbf{x}_0 &\sim \mathcal{N}(c_t \cdot \mathbf{x}_0, d_t^2 \cdot \mathbf{I}_{d_x}) \\
\mathbf{Y}_t \mid \mathbf{Y}_0 = \mathbf{y}_0 &\sim \delta(\mathbf{y}_t - c_t \cdot \mathbf{y}_0) \\
\mathbf{Y}_0 \mid \mathbf{X}_0 = \mathbf{x}_0 &\sim \mathcal{N}(A\mathbf{x}_t, \sigma_y^2 \mathbf{I}_{d_y})
\end{aligned}$$

We have:

$$\begin{aligned}
\mathbb{E}\left\{\mathbf{Y}_t \mid \mathbf{X}_0\right\} &= \mathbb{E}\left\{\mathbb{E}\left\{\mathbf{Y}_t \mid \mathbf{Y}_0\right\} \mid \mathbf{X}_0\right\} \\
&= \mathbb{E}\left\{c_t \cdot \mathbf{Y}_0 \mid \mathbf{X}_0\right\} \\
&= c_t \cdot A\mathbf{X}_0
\end{aligned}$$

and

$$\begin{aligned}
\mathbb{V}\left\{\mathbf{Y}_t \mid \mathbf{X}_0\right\} &= \mathbb{E}\left\{\mathbb{V}\left\{\mathbf{Y}_t \mid \mathbf{Y}_0\right\} \mid \mathbf{X}_0\right\} + \mathbb{V}\left\{\mathbb{E}\left\{\mathbf{Y}_t \mid \mathbf{Y}_0\right\} \mid \mathbf{X}_0\right\} \\
&= \mathbb{V}\left\{c_t \cdot \mathbf{Y}_0 \mid \mathbf{X}_0\right\} \\
&= c_t^2 \sigma_y^2 \cdot \mathbf{I}_{d_y}
\end{aligned}$$

Hence:

$$\mathbf{Y}_t \mid \mathbf{X}_0 = \mathbf{x}_0 \sim \mathcal{N}(c_t \cdot A\mathbf{x}_0, \sigma_y^2 c_t^2 \cdot \mathbf{I}_{d_y})$$

Further:

$$\begin{aligned}
& A\mathbf{X}_t \mid \mathbf{X}_0 = \mathbf{x}_0 \sim \mathcal{N}(c_t \cdot A\mathbf{x}_0, d_t^2 \cdot AA^\top) \\
\implies & \mathbf{Y}_t - A\mathbf{X}_t \mid \mathbf{X}_0 = \mathbf{x}_0 \sim \mathcal{N}(0, \sigma_y^2 c_t^2 \cdot \mathbf{I}_{d_y} + d_t^2 \cdot AA^\top) \\
\implies & \mathbf{Y}_t \mid \mathbf{X}_t = \mathbf{x}_t \sim \mathcal{N}(A\mathbf{x}_t, \sigma_y^2 c_t^2 \cdot \mathbf{I}_{d_y} + d_t^2 \cdot AA^\top)
\end{aligned}$$

□

Proposition B.1 (Gaussian-Gaussian Exactness for Linear Observations)**.** Suppose

$$\begin{aligned}\mathbf{X}_t \mid \mathbf{X}_{t+1} &\sim \mathcal{N}\left(\mu_{t+1}(\mathbf{x}_{t+1}), \Sigma_{t+1}\right)\\ \mathbf{Y}_t \mid \mathbf{X}_t = \mathbf{x}_t &\sim \mathcal{N}\left(A\mathbf{x}_t, \Xi_t\right)\end{aligned}$$

Consider some proposal:

$$p_t(\mathbf{x}_t \mid \mathbf{y}_t, \mathbf{x}_{t+1}) \propto p_t(\mathbf{x}_t \mid \mathbf{x}_{t+1}) g_t(\mathbf{y}_t \mid \mathbf{x}_t)$$

Then:

$$\mathbf{Y}_t \mid \mathbf{X}_{t+1} = \mathbf{x}_{t+1} \sim \mathcal{N}\left(A\mu_{t+1}, \Xi_t + A\Sigma_{t+1}A^\top\right)$$

Proof. By Gaussian conjugacy, it immediately follows that:

$$\mathbf{X}_t \mid \mathbf{Y}_t = \mathbf{y}_t, \mathbf{X}_{t+1} = \mathbf{x}_{t+1} \sim \mathcal{N}\left(\mu_{t+1}^P, \Sigma_{t+1}^P\right)$$

where

$$\begin{aligned}\mu_{t+1}^P &= \Sigma_{t+1}^P\left(\Sigma_{t+1}^{-1}\mu_{t+1}(\mathbf{x}_{t+1}) + A^\top \Xi_t^{-1}\mathbf{y}_t\right)\\ \Sigma_{t+1}^P &= \left(\Sigma_{t+1}^{-1} + A^\top \Xi_t^{-1} A\right)^{-1}\end{aligned}$$

The normalizing constant of the proposal is:

$$\int p_t(\mathbf{x}_t \mid \mathbf{x}_{t+1}) g_t(\mathbf{y}_t \mid \mathbf{x}_t)\, d\mathbf{x}_t = g_t(\mathbf{y}_t \mid \mathbf{x}_{t+1})$$

Note that:

$$\begin{aligned}
\mathbb{E}\left\{\mathbf{Y}_t \mid \mathbf{X}_{t+1}\right\} &= \mathbb{E}\left\{\mathbb{E}\left\{\mathbf{Y}_t \mid \mathbf{X}_t\right\} \mid \mathbf{X}_{t+1}\right\} && \dots \text{tower property} \\
&= \mathbb{E}\left\{A\mathbf{X}_t \mid \mathbf{X}_{t+1}\right\} \\
&= A\mathbb{E}\left\{\mathbf{X}_t \mid \mathbf{X}_{t+1}\right\} \\
&= A\mu_{t+1}(\mathbf{X}_{t+1}) \\
\mathbb{V}\left\{\mathbf{Y}_t \mid \mathbf{X}_{t+1}\right\} &= \mathbb{E}\left\{\mathbb{V}\left\{\mathbf{Y}_t \mid \mathbf{X}_t\right\} \mid \mathbf{X}_{t+1}\right\} + \mathbb{V}\left\{\mathbb{E}\left\{\mathbf{Y}_t \mid \mathbf{X}_t\right\} \mid \mathbf{X}_{t+1}\right\} && \dots \text{total variance} \\
&= \mathbb{E}\left\{\Xi_t \mid \mathbf{X}_{t+1}\right\} + \mathbb{V}\left\{A\mathbf{X}_t \mid \mathbf{X}_{t+1}\right\} \\
&= \Xi_t + A\mathbb{V}\left\{\mathbf{X}_t \mid \mathbf{X}_{t+1}\right\} A^\top \\
&= \Xi_t + A\Sigma_{t+1}A^\top
\end{aligned}$$

Since $\mathbf{Y}_t$ is an affine transformation, it follows then that:

$$\mathbf{Y}_t \mid \mathbf{X}_{t+1} = \mathbf{x}_{t+1} \sim \mathcal{N}\left(A\mu_{t+1}, \Xi_t + A\Sigma_{t+1}A^\top\right)$$

□

C. Further Experimental Details

Gaussian Mixture Model We initially aimed to include MCGdiff (Cardoso et al., 2023) in our comparison. However, we were unable to reproduce their results, even using the code on their repository. Indeed, we found that the resulting sliced Wasserstein distances from MCGdiff were almost uniformly larger (worse) than those of SMCDiffOpt on each experimental run (i.e. given identical setups and pseudo-RNG seeds). This is doubly unexpected since the results we were seeing don't align with those found in their paper, and since theoretically their proposal should be more optimal than ours for this particular task; if we take the values they give in Table 1 of their paper and compare them with those in Table 4.1 we see this is indeed the case. Given the time constraints, the exhaustion of all obvious potential author-errors, and assuming the validity of their results, we opted to omit our results from a comparison. For posterity, we provide in Table C.2 the results including MCGdiff but note with caution that we lack confidence in such figures.

Branin Optimization **TODO**: Model architecture description...

σ_y	d_x	d_y	SMCDiffOpt	MCGDiff	DPS	ΠGD	TMPD
0.0	8	1	0.98 ± 0.44	0.95 ± 0.44	8.22 ± 7.32	3.15 ± 2.58	3.5 ± 2.67
		2	0.55 ± 0.43	0.39 ± 0.33	0.41 ± 0.29	0.33 ± 0.27	0.44 ± 0.34
		4	0.21 ± 0.07	0.15 ± 0.09	0.12 ± 0.06	0.09 ± 0.03	0.08 ± 0.04
	80	1	0.75 ± 0.31	1.06 ± 0.77	2.45 ± 1.79	3.18 ± 2.6	2.66 ± 1.47
		2	1.22 ± 1.04	2.31 ± 2.21	1.35 ± 1.21	0.33 ± 0.27	0.81 ± 0.68
		4	0.26 ± 0.05	2.22 ± 1.92	0.97 ± 0.86	0.08 ± 0.02	0.68 ± 0.44
0.1	8	1	1.13 ± 0.51	0.79 ± 0.62	8.18 ± 7.5	3.22 ± 2.67	3.11 ± 2.31
		2	0.2 ± 0.07	1.15 ± 1.09	0.38 ± 0.28	0.19 ± 0.13	0.43 ± 0.34
		4	0.15 ± 0.05	0.25 ± 0.12	0.16 ± 0.06	0.07 ± 0.01	0.06 ± 0.01
	80	1	1.25 ± 1.02	1.26 ± 0.87	2.51 ± 2.11	2.93 ± 2.56	2.56 ± 1.18
		2	0.45 ± 0.32	3.06 ± 2.93	1.27 ± 1.14	0.62 ± 0.56	0.66 ± 0.54
		4	0.23 ± 0.06	3.34 ± 3.01	1.03 ± 0.9	0.08 ± 0.02	0.63 ± 0.34
1.0	8	1	1.35 ± 1.0	1.14 ± 0.7	6.62 ± 4.96	1.16 ± 0.72	1.35 ± 0.9
		2	0.44 ± 0.28	1.11 ± 1.04	2.92 ± 2.42	0.94 ± 0.89	1.44 ± 1.15
		4	0.15 ± 0.03	0.12 ± 0.06	1.19 ± 0.66	0.1 ± 0.03	0.45 ± 0.26
	80	1	1.69 ± 1.37	1.49 ± 0.75	5.26 ± 4.4	1.2 ± 0.79	1.23 ± 0.53
		2	0.89 ± 0.78	2.08 ± 1.97	3.21 ± 2.95	1.68 ± 1.62	1.41 ± 1.16
		4	1.12 ± 0.92	4.52 ± 2.55	1.54 ± 0.99	0.89 ± 0.74	1.37 ± 0.67

Table C.2.: Sliced-Wasserstein distances for GMM experiment with MCGdiff included. These results do not align with those in Cardoso et al. (2023), despite running exactly the script in their repository.

D. Additional Background and Related Works

Diffusion Models

Remark D.1 (SDE Representation)**.** The DDPM approach corresponds to a discretized time rescaled Ornstein-Uhlenbeck process (Boys et al., 2023; Y. Song et al., 2021):

$$d\mathbf{x}_t = -\frac{1}{2}\beta(t)\mathbf{x}_t dt + \sqrt{\beta(t)}d\mathbf{w}_t$$

and is often referred to as the variance-preserving SDE (Y. Song et al., 2021). Going forwards, we will stick to the Markov (discretised) representation, but ultimately they are equivalent when it comes to sampling. This point is worth noting though as the SDE representation is what analytically justifies the backwards process (see footnote 1).

Remark D.2 (DDIM Representation)**.** Under DDIM:

$$u_t = \sqrt{\alpha_{t-1}} \quad v_t = -\sqrt{1-\overline{\alpha}_{t-1}-\sigma_t^2}\sqrt{1-\overline{\alpha}_t} \quad w_t = \sigma_t$$

with $\{\sigma_t\}_{t=1}^T$ an arbitrary conditional variance sequence. It's common to consider:

$$\sigma_t(\eta) = \eta\sqrt{\frac{1-\alpha_{t-1}}{1-\alpha_t}}\sqrt{1-\frac{\alpha_t}{\alpha_{t-1}}}, \quad \eta \in [0,1]$$

with $\eta = 1$ ultimately reducing u_t, v_t, w_t to the DDPM values, and $\eta = 0$ corresponding to deterministic generation (J. Song et al., 2020).

Remark D.3 (Time Respacing)**.** One of the remarkable features of the DDIM algorithm is it enabling *time re-spacing* whereby we can sample from the backwards process in fewer time-steps. In this paper, we don't consider such re-spacing though in principle our methodology does not prohibit it.

FPS-SMC Rather than Equation 19, Dou and Song (2023) instead considers a "shared-noise" or "duplex" diffusion:

Proposition D.1 (Obvservation Diffusion)**.** Dou and Song (2023, Proposition B.1). Let $\mathbf{x}_t$ be generated according to the forward marginal of some diffusion process. Let $\mathbf{y} = \mathbf{y}_0$ be some (linear) measurement we have about the clean sample, $\mathbf{x}_0$. Construct a sequence $\{\mathbf{y}_t\}_{t=1}^T$ by:

$$\mathbf{y}_t = a_t \cdot \mathbf{y}_{t-1} + b_t \cdot A\epsilon_t, \quad \epsilon_t \sim \mathcal{N}(0, \mathbf{I}_{d_y})$$

where ϵ_t is the *same* as used for forward noising $\mathbf{x}_0$ at time-step t. It follows that:

$$\mathbf{Y}_t \mid \mathbf{X}_t = \mathbf{x}_t \sim \mathcal{N}(A\mathbf{x}_t, \sigma_y^2 c_t^2 \cdot \mathbf{I}_{d_y}) \tag{24}$$

with $g(\mathbf{y}_0 \mid \mathbf{x}_0) = g(\mathbf{y} \mid \mathbf{x}_0) = \mathcal{N}(\mathbf{y}; A\mathbf{x}_0, \sigma_y^2 \cdot \mathbf{I}_{d_y})$ exactly the measurement density.

Note because of the noise-sharing, we get cancellation in the covariance of the likelihood, dropping the $d_t^2 \cdot AA^\top$ term as in Equation 20.

Based on Proposition D.1 and Dou and Song (2023, Remark B.1), we can generate some $\{\mathbf{y}_t\}_{t=0}^T$ either forwards or *backwards*. The latter follows because where in the backwards process for $\mathbf{x}_t$ we use an estimate of $\mathbf{x}_0$ (via Tweedie's formula), for the observations we have $\mathbf{y}_0$, and an expression can be analytically derived.